Advanced Composite Materials
Publication details, including instructions for authors and subscription information:
http://www.tandfonline.com/loi/tacm20

Molecular Dynamics Simulation of Elastic Properties and Fracture Behavior of Single Wall Carbon Nanotubes with Vacancy and Stone-Wales Defect

Keka Talukdar [a] & A. K. Mitra [b]

[a] Department of Physics, National Institute of Technology, Durgapur-713209, India

[b] Department of Physics, National Institute of Technology, Durgapur-713209, India

Version of record first published: 02 Apr 2012.

To cite this article: Keka Talukdar & A. K. Mitra (2011): Molecular Dynamics Simulation of Elastic Properties and Fracture Behavior of Single Wall Carbon Nanotubes with Vacancy and Stone-Wales Defect, Advanced Composite Materials, 20:1, 29-38

To link to this article: http://dx.doi.org/10.1163/092430410X504189

VSP

Advanced Composite Materials 20 (2011) 29–38

ADVANCED COMPOSITE MATERIALS
brill.nl/acm

Molecular Dynamics Simulation of Elastic Properties and Fracture Behavior of Single Wall Carbon Nanotubes with Vacancy and Stone–Wales Defect

Keka Talukdar and A. K. Mitra *

Department of Physics, National Institute of Technology, Durgapur-713209, India

Received 22 September 2009; accepted 6 November 2009

Abstract

Perfect carbon nanotubes are exceptionally strong nanostructures with fascinating mechanical characteristics. But the presence of crystal defects like Stone–Wales defects or vacancies degrade their mechanical properties to a large extent. The effects of the presence of a single Stone–Wales defect or a single vacancy defect on the elastic properties and the fracture pattern of a single-walled carbon nanotube (SWCNT) are investigated by molecular dynamics (MD) simulation. We considered three samples of SWCNT, one each of chiral, armchair and zigzag type. In all the three samples, significant changes are observed compared to a defect-free tube. A defective chiral (10,6) tube shows more stability under stretched condition compared to the armchair (7,7) or the zigzag (10,0) tube as revealed from the energy differences between defective and defect-free tubes at different stages of deformation. Fluctuation of energy differences for higher strain values for the same defect orientation is observed to be most pronounced in the case of a zigzag tube and hence shows a less stable configuration than the other two tubes. The fracture pattern in each case is modelled and shows that defects play a major role in the breaking mechanism of a SWCNT. Also the differences in fracture modes of chiral and achiral tubes prove the dependence of their mechanical behavior on chirality.

Keywords

MD simulation, SWCNT, mechanical properties, fracture, SW defect

1. Introduction

Using carbon nanotubes (CNTs) as reinforcing agents to design and fabricate strong composites with desirable mechanical properties needs thorough understanding of the mechanical behavior of such nanotubes. Topological defects such as Stone–Wales (SW) [1] defects or vacancies that are inherently present in the CNTs or introduced into them in the manufacturing process greatly degrade their mechanical properties. Although many theoretical and experimental studies have been carried

* To whom correspondence should be addressed. E-mail: akmrecdgp@yahoo.com
Edited by JSCM

DOI:10.1163/092430410X504189

out to explore the mechanical behavior of carbon nanotubes, a wide variation in their results has been reported so far showing the theoretical values to be generally higher than the experimental ones. Theoretical studies [2–7] show a wide range of Young's modulus values from 0.1 to 5.5 TPa, while the calculated tensile strength varies from 5 to 150 GPa, depending on the method of calculation, CNT chiralities and the potentials employed to define the C–C bond in the plane of the graphene sheet. The bending and buckling of CNTs under large strains are shown in the experimental work of Falvo *et al*. [8]. Theoretically overestimated values of nanotube properties can be attributed to the presence of various defects in the CNT structures.

The role of vacancy defects or holes on the mechanical properties of CNTs was studied in many theoretical investigations such as by Mielke *et al*. [9], Lee *et al*. [10], Xiao and Hou [11] and Wang *et al.* [12]. In the Molecular Mechanics (MM) and Molecular Dynamics (MD) study of Belytschko *et al*. [13], the effects of missing atoms and SW defects on the failure pattern were studied. In their study, Young's modulus showed very little dependence on the presence of SW defects. Their results were in good agreement with the experimental observations of Yu *et al*. [14] for Morse potential but not for Brenner potential. Somewhat higher values than the observations of Yu *et al*. were obtained by Mielke *et al.* [9] who observed a 20–30% reduction of strain values by MM calculation and 14–27% reduction by Quantum Mechanical (QM) calculation for vacancy defects. Troya *et al*. [15], Chandra *et al*. [16] and Lu and Bhattacharya [17], observed in their calculations the effects of SW defects on the stiffness and maximum strain. Tserpes and Papanikos [18] used pairwise modified Morse potential to come to the conclusion that SW defects served as nucleation site for fracture. They also observed reduction in failure stress and strain for different types of nanotubes where armchair nanotubes exhibited the largest reduction of failure stress of 18–25% with reduction in failure strain value of 30–41%. Tight Binding MD simulation was carried out by Richard *et al.* [19] who studied the effects of various defects including SW defects. Recently, using Tersoff–Brenner potential, Pozrikidis [20] has studied the effects of circumferential as well as inclined SW defects. Necking phenomenon was reported by them and the fracture of the tube in each case was found to be brittle.

As Stone–Wales defect and vacancy defect are the two major kinds of defects in SWCNTs, their effects are investigated and compared in our study using the bond order potential. Most of the earlier authors used the modified Morse potential in their simulation study; but the whole process of straining can be studied properly only with the bond order potential. In the present work, three different types of SWCNTs are subjected to increasing axial strain and various mechanical characteristics are computed and their fracture mechanisms modeled, with and without defects. As the CNTs can serve as reinforcing agents for making strong composites, the detailed study of their mechanical strength and fracture behavior is essential.

2. Method of Calculation

We have used the interatomic potential function developed by Brenner [21] for hydrocarbons, known as the Tersoff–Brenner bond order potential. Though it does not include long range molecular interaction, it enables us to simulate a wide range of deformations of a CNT under external loads. Due to the presence of a cut-off function, this pair potential includes the contribution of the near neighbors only.

Using the above potential interatomic interaction, MD simulation is carried out on an armchair (7,7), a zigzag (10,0) and a chiral (10,6) single-walled carbon nanotube (SWCNT) with aspect ratios of 10.36, 10.88 and 10.88, respectively. Keeping one end fixed, axial tensile force is applied on the other end of the tube. A Berendsen thermostat is used to allow small changes in the velocities of the atoms such that the temperature of the system reaches a preassigned equilibrium value. Temperature is controlled by the thermostat and set at 300 K. At first, the defect-free tubes are stretched up to failure. Then one vacancy defect and one SW defect are separately introduced into them at $z = 0$. The force in the lateral direction is set equal to zero while the tube is strained longitudinally. Stress is calculated from the energy–strain curve according to the relation $\sigma = 1/A(\mathrm{d}E/\mathrm{d}\varepsilon)$, where σ is the stress, A is the area of the annular cross-section of the tube and $(\mathrm{d}E/\mathrm{d}\varepsilon)$ is the slope of the energy–strain curve, where ε represents the strain. Area of the annular cross-section of the tube is found as $A = 2\pi r\delta r$, where r is the radius of the tube and δr is its wall thickness, taken as 0.34 nm which has now become the standard value for SWCNT. Young's modulus (Y) is found from the slope of the linear portion of the curve.

3. Results and Discussion

We first considered the defect-free tubes and stretched them up to failure. Strain is defined as $\varepsilon = (L - L_0)/L_0$, where L_0 and L are the initial and stretched length of the tube. The strain energy for a defect free (7,7) SWCNT drops sharply at 32% strain (Fig. 1) giving a tensile strength of 161.2 GPa. Our interest is in the room temperature behavior of the samples where the distribution of kinetic energy of the atoms follows the Boltzmann distribution law; so at that temperature some bonds may be stretched beyond the point of maximum stress. The black line in Fig. 1 shows this very well where the maximum sustainable strain goes up to 32%, which is the actual failure strain. Before that the tube shows some ductility. Young's modulus for a perfect (7,7) tube is found to be 0.893 TPa. This Young's modulus value is slightly lower than the experimentally obtained average value of 1.5 TPa for SWCNTs by Krishnan *et al*. [22]. Our results are close to the experimental results of Wong *et al.* [23] and Treacy *et al.* [24] also. Failure stress values can be compared with the experimental values of 150 ± 45 GPa obtained by Demczyk [25]. Quantum mechanical calculations [7, 15, 26] have also given the failure stress values of more than 100 GPa and predicted the maximum strain values between 20%

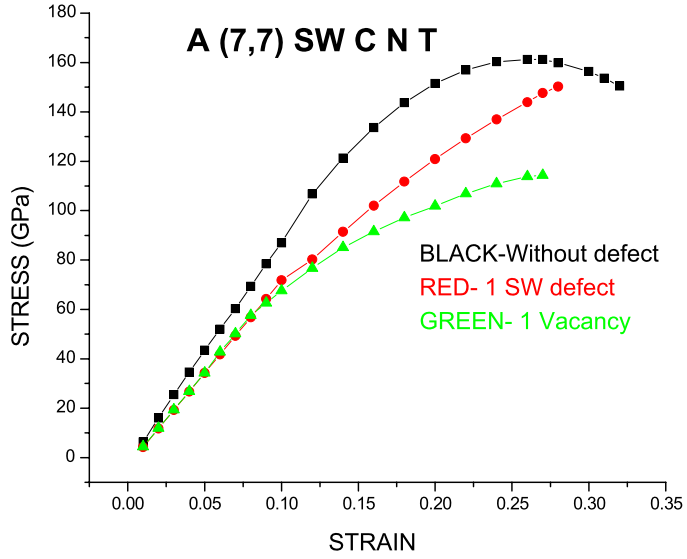

Figure 1. Stress–strain curves for a (7,7) SWCNT. This figure is published in color on http://www.ingentaconnect.com/content/vsp/acm

to 30%, which are comparable to our results. In computer simulation, large values of maximum strain are usually obtained as in the straining procedure; the system does not get sufficient time to come back to a relaxed state.

Introduction of one SW defect at the mid-position changes the tube structure locally where pentagons, created by 90° rotation of the bond, orient themselves along the stretching direction. Reduction of maximum strain is 18.75% (Fig. 1) as armchair symmetry reduces the strain energy of the defective tube by elongation of length along the direction where pentagons are formed, which is also the direction of the force. The presence of a single vacancy however reduces the maximum strain by 15.6% (Fig. 1). For the same reason, for armchair symmetry, the difference in energy between the tube with SW defect and without any defect, shows stability for larger strains (Fig. 2). Less stable bonds are observed due to vacancy defect where the said difference drops after 14% strain. The armchair defect-free tube breaks near the end where the force is applied (Fig. 3(a)). This part is axially displaced due to the application of the force and most of the bonds of that part are broken. For defective tubes, breaking starts from the defect sites (Fig. 3(b) and 3(c)).

A zigzag (10,0) SWCNT without defect exhibits a maximum tensile strength of 115.4 GPa and the maximum strain of 18% (Fig. 4). Reduction of maximum strain is observed with a single vacancy. Stress–strain curves for defect-free and defective tubes are shown in Fig. 4. Zigzag symmetry does not help the tube to release the excess strain in the loading direction as the two pentagons formed are not in the loading direction, but inclined with the tube axis. So, maximum strain for the same tube with a SW defect is 17% (Fig. 4). Greater resistance to the applied force is

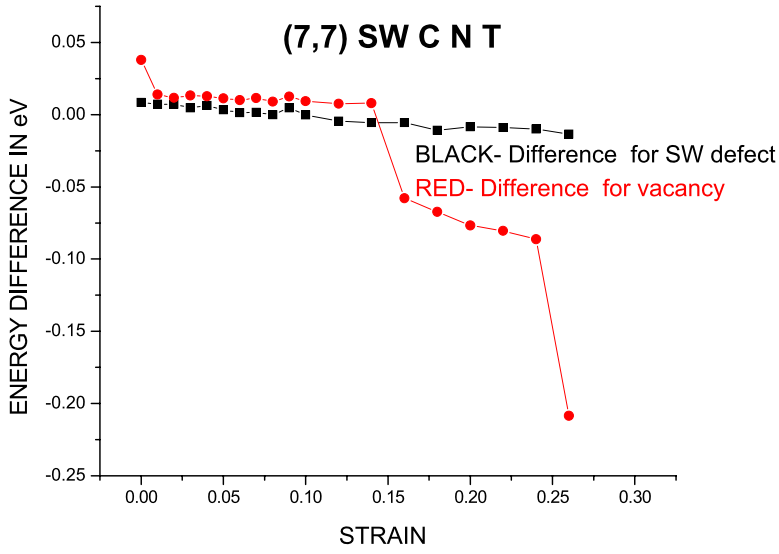

Figure 2. Difference of energy between a defect-free (7,7) tube and a tube with 1 SW defect or 1 vacancy defect at different strains. This figure is published in color on http://www.ingentaconnect.com/content/vsp/acm

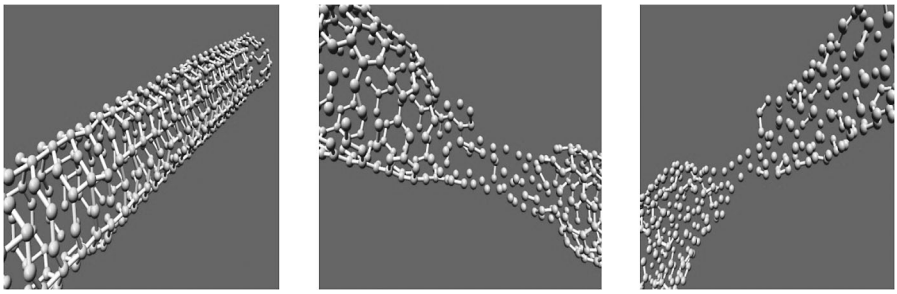

Figure 3. Fracture pattern of a defect-free (7,7) SWCNT (a), with 1 SW defect (b) and with one vacancy defect (c).

given by the tube in the axial direction. The energy differences between the perfect and imperfect tubes for increasing strains (Fig. 5) are different in character from those in Fig. 2. Fluctuation starts from 14% strain, which increases for large strain. So, a zigzag tube is less stable under defective condition. As stress–strain curves show sudden drops after the inflection points, the fracture in all cases can be said to be brittle. Rapid breaking of bonds is observed from Fig. 6.

The inflection point occurs at 24% strain for a perfect (10,6) SWCNT (Fig. 7). Maximum strain undergoes very little change by the inclusion of SW defect, but with vacancy defect, no such change is observed (Table 1). The more stable configuration of (10,6) SWCNT compared to the other two tubes (Fig. 8) is observed

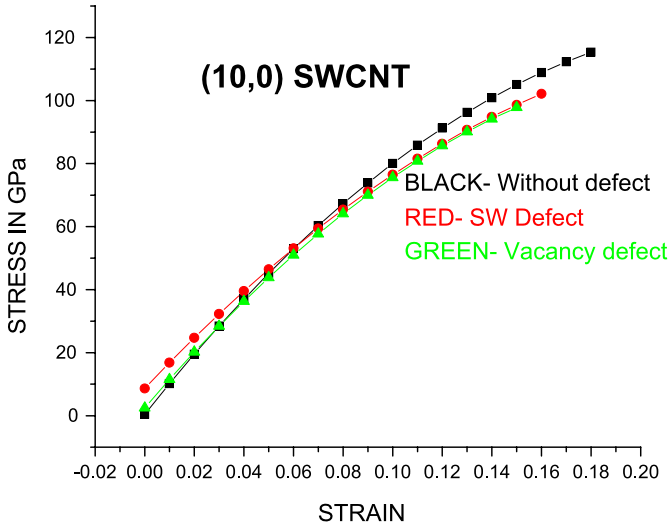

Figure 4. Stress–strain curves for a (10,0) SWCNT. This figure is published in color on http://www.ingentaconnect.com/content/vsp/acm

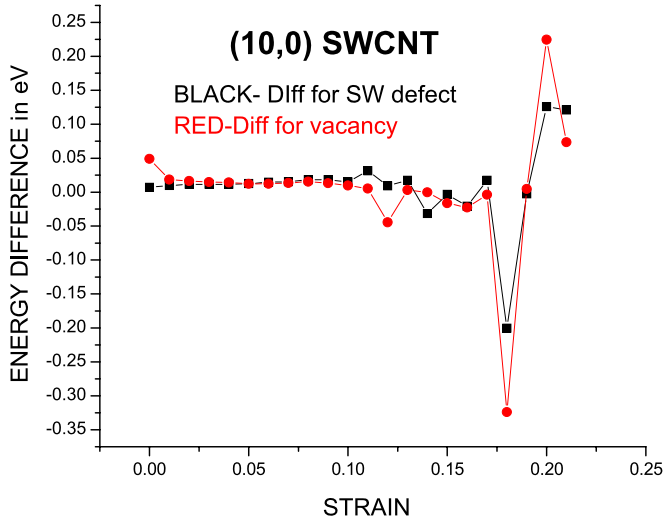

Figure 5. Difference of energy between a defect-free (10,0) tube and a tube with 1 SW defect or 1 vacancy defect for different strains. This figure is published in color on http://www.ingentaconnect.com/content/vsp/acm

when the defects are introduced into it. The pristine tube breaks at the end (Fig. 9(a)) while the defective tubes break from the defective region. But looking at Fig. 9 it can be concluded that fracture of defective tubes are not brittle in character but certainly stretching is not possible beyond the maximum strain as several bonds are displaced from their proper position and also many bonds are broken.

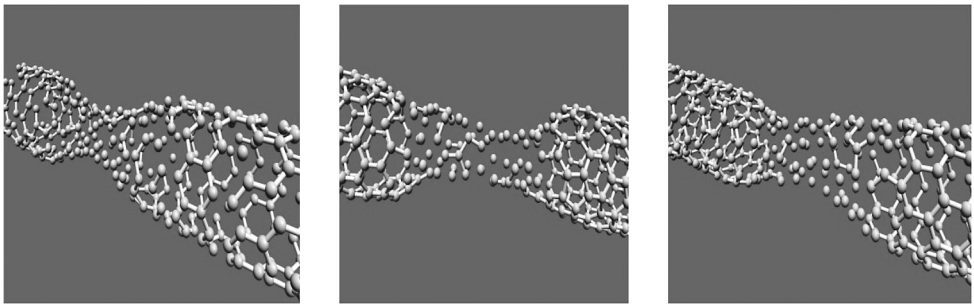

Figure 6. Breaking behaviors of a defect-free (10,0) SWCNT (a), with 1 SW defect (b) and with one vacancy defect (c).

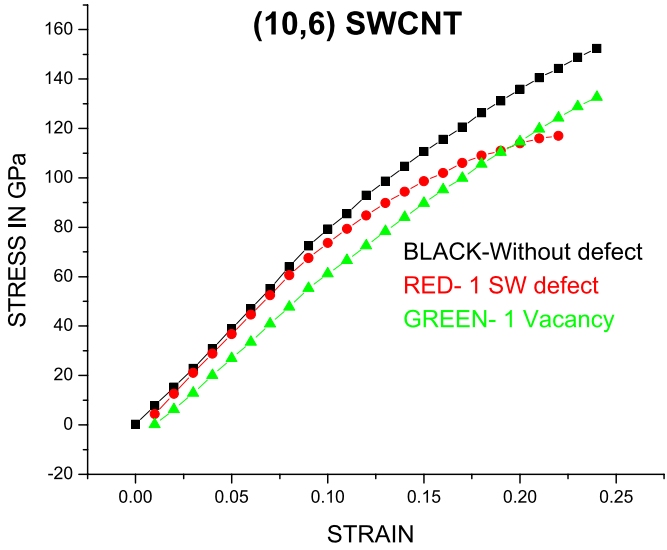

Figure 7. Stress–strain curves for a (10,6) SWCNT. This figure is published in color on http://www.ingentaconnect.com/content/vsp/acm

Table 1.
Variation of the calculated values of the mechanical characteristics of the SWCNT with and without defects

SWCNT	Without defect			1 SW defect			1 vacancy defect		
	*Y.M. (TPa)	T.S. (GPa)	M.S. (%)	Y.M. (TPa)	T.S. (GPa)	M.S. (%)	Y.M. (TPa)	T.S. (GPa)	M.S. (%)
Armchair (7,7)	0.893	161.2	32	0.75	150.2	26	0.764	114.4	27
Zigzag (10,0)	0.895	115.4	18	0.832	105.3	17	0.845	97.8	16
Chiral (10,6)	0.809	152.4	24	0.799	117	22	0.69	132.7	24

*Y.M. — Young's modulus, T.S. — tensile strength, M.S. — maximum strain.

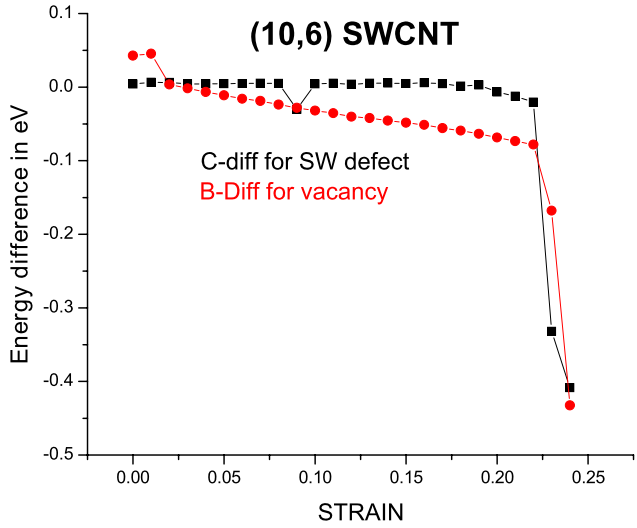

Figure 8. Difference of energy between a defect-free tube (10,6) and tubes with 1 SW defect and 1 vacancy defect for different strains. This figure is published in color on http://www.ingentaconnect.com/content/vsp/acm

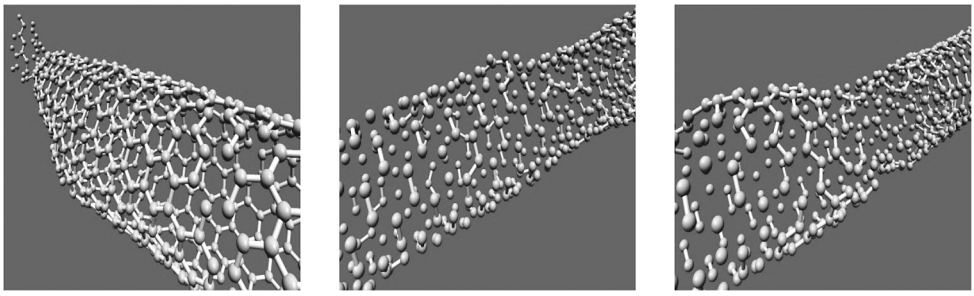

(a) (b) (c)

Figure 9. Fracture behavior of a defect-free (10,6) SWCNT (a), with 1 SW defect (b) and with one vacancy defect (c).

4. Conclusions

By MD simulation analysis of the three types of SWCNTs without defect and with a single SW defect or a single vacancy defect, we have obtained an overall picture of the degradation of all mechanical properties of the SWCNTs with the inclusion of defects. An armchair tube with a vacancy and a chiral tube with one SW defect show 29.3% and 23.2% reduction in tensile strength, respectively. In spite of this a chiral tube with defects shows maximum stability while straining. Young's moduli of the tubes are also affected by 16% for an armchair tube with 1 SW defect and by 14% for a chiral tube with a vacancy defect. Remarkable changes in ductility are observed for an armchair tube where 18.75% and 15.65% reductions are noticed

with a SW defect and vacancy defect, respectively. But in our calculation very little change in ductility is observed for the other two tubes. Fracture is brittle for the armchair and zigzag tubes but for a chiral tube the fracture is not so prominent.

References

1. A. J. Stone and D. J. Wales, Theoretical studies of icosahedral C60 and some related species, *Chem. Phys. Lett*. **128**, 501–503 (1986).
2. B. I. Yakobson, C. J. Brabec and J. Bernholc, Nanomechanics of carbon tubes: instabilities beyond linear response, *Phys. Rev. Lett*. **76**, 2511–2514 (1996).
3. B. I. Yakobson, Mechanical relaxation and intramolecular plasticity in carbon nanotubes, *Appl. Phys. Lett*. **72**, 918–920 (1998).
4. K. M. Liew, C. H. Wong, X. Q. He, M. J. Tan and S. A. Meguid, Nanomechanics of single and multiwalled carbon nanotubes, *Phys. Rev*. **B 69**, 1–8 (2004).
5. R. C. Batra and A. Sears, Uniform radial expansion/contraction of carbon nanotubes and their tranverse elastic moduli, *Modelling Simul. Mater. Sci. Engng* **15**, 835–844 (2007).
6. V. R. Coluci, N. M. Pugno, S. O. Dantas, D. S. Galvao and A. Jorio, Atomistic simulations of the mechanical properties of 'super' carbon nanotubes, *Nanotechnology* **18**, 1–7 (2007).
7. G. Dereli and C. Ozdogan, Structural stability and energetics of single-walled carbon nanotubes under uniaxial strain, *Phys. Rev*. **B 67**, 1–6 (2003).
8. M. R. Falvo, G. J. Clary, R. M. Taylor, V. Chi, F. P. Brooks Jr., S. Washburn and R. Superfine, Bending and buckling of carbon nanotubes under large strain, *Nature* **389**, 582–584 (1997).
9. S. L. Mielke, D. Troya, S. Zhang, J. L. Li, R. C. Xiao and R. S. Ruoff, The role of vacancy defects and holes in the fracture of carbon nanotubes, *Chem. Phys. Lett*. **390**, 413–420 (2004).
10. G. D. Lee, C. Z. Wang, E. Yoon, N. M. Hwang and K. M. Ho, Vacancy defects and the formation of local haecklite structures in graphene from tight-binding molecular dynamics, *Phys. Rev*. **B 74**, 1–5 (2006).
11. S. P. Xiao and W. Y. Hou, Mechanical behaviors of carbon nanotubes with randomly located vacancy defects, *J. Nanosci. Nanotech*. **7**, 1–8 (2007).
12. Q. Wang, W. H. Duan, N. Richards and K. M. Liew, Modeling of fracture of carbon nanotubes with vacancy defects, *Phys. Rev*. **B 75**, 1–4 (2007).
13. T. Belytschko, S. P. Xiao, G. C. Schatz and R. Ruoff, Atomistic simulations of nanotube fracture, *Phys. Rev*. **B 65**, 1–8 (2002).
14. M. F. Yu, B. S. Files, S. Arepalli and R. S. Ruoff, Tensile loading of ropes of single wall carbon nanotubes and their mechanical properties, *Phys. Rev. Lett*. **84**, 5552–5555 (2000).
15. D. Troya, S. L. Mielke and G. C. Schatz, Carbon nanotube fracture-differences between quantum mechanical mechanisms and those of empirical potentials, *Chem. Phys. Lett*. **382**, 133–141 (2003).
16. N. Chandra, S. Namilae and C. Shet, Local elastic properties of carbon nanotubes in the presence of Stone–Wales defects, *Phys. Rev*. **B 69**, 1–12 (2004).
17. Q. Lu and B. Bhattacharya, Effect of randomly occurring Stone–Wales defects on mechanical properties of carbon nanotubes using atomistic simulation, *Nanotechnology* **16**, 5550–5566 (2005).
18. K. I. Tserpes and P. Papanikos, The effect of Stone–Wales defect on the tensile behavior and fracture of single-walled carbon nanotubes, *Compos. Struct*. **79**, 581–589 (2007).
19. W. H. Richard, S. M. Robert, M. E. Robert, P. M. Charles, L. M. Dustin, J. B. Anthony, R. W. Charles, C. B. Bruce and T. W. David, Tight-binding molecular dynamics study of

the role of defects on carbon nanotube moduli and failure, *J. Chem. Phys*. **127**, 074708, DOI:10.1063/1.2756832 (2007).
20. C. Pozrikidis, Effect of the Stone–Wales defect on the structure and mechanical properties of single-wall carbon nanotubes in axial stretch and twist, *Arch. Appl. Mech.* **79**, 113–123, DOI 10.1007/s00419-008-0217-6 (2009).
21. D. W. Brenner, Empirical potential for hydrocarbons for use in simulating the chemical vapour deposition of diamond films, *Phys. Rev.* **B 42**, 9458–9471 (1990).
22. A. Krishnan, E. Dujardin, T. W. Ebbesen, P. N. Yianilos and M. M. J. Treacy, Young's modulus of single-walled nanotubes, *Phys. Rev.* **B 58**, 14013–14019 (1998).
23. E. W. Wong, P. E. Sheehan and C. M. Lieber, Nanobeam mechanics: elasticity, strength and toughness of nanorods and nanotubes, *Science* **277**, 1971–1975 (1997).
24. M. M. J. Treacy, T. W. Ebbesen and J. M. Gibson, Exceptional high Young's modulus observed for individual carbon nanotubes, *Nature* **381**, 678–680 (1996).
25. B. G. Demczyk, Direct mechanical measurement of the tensile strength and elastic modulus of multiwalled carbon nanotubes, *Mater. Sci. Engng* **A 334**, 173–178 (2002).
26. T. Ozaki, Y. Iwasa and T. Mitani, Stiffness of single-walled carbon nanotubes under large strain, *Phys. Rev. Lett*. **84**, 1712–1715 (2000).